International Journal of Nanomedicine

Dovepress
open access to scientific and medical research

Open Access Full Text Article

ORIGINAL RESEARCH

Immobilized transferrin Fe_3O_4@SiO_2 nanoparticle with high doxorubicin loading for dual-targeted tumor drug delivery

This article was published in the following Dove Press journal:
International Journal of Nanomedicine
2 December 2013
Number of times this article has been viewed

Wence Ding
Lin Guo

Key Laboratory of Mesoscopic Chemistry of Ministry of Education, School of Chemistry and Chemical Engineering, Nanjing University, Nanjing, People's Republic of China

Abstract: Transferrin (Tf) was immobilized onto Fe_3O_4@SiO_2 nanoparticles with high doxorubicin (DOX) loading (TfDMP), for dual targeting of cancer, by chemically coupling both Tf and DOX with dual-function magnetic nanoparticles (DMPs) using a multi-armed crosslinker, poly-L-glutamic acid. With high trapping efficiency for magnetic targeting, TfDMP exhibits a Tf receptor-targeting function. Moreover, the DOX loading percentage of TfDMP is high, and can be controlled by adjusting the reactant ratio. TfDMP presents a narrow size distribution, and is sensitive to pH for drug release. Compared with DOX-coupled DMP without Tf modification (DDMP), TfDMP exhibits enhanced uptake by Tf receptor-expressing tumor cells, and displays stronger cancer cell cytotoxicity. This study provides an efficient method for the dual-targeted delivery of therapeutic agents to tumors, with controlled low carrier toxicity and high efficiency.

Keywords: transferrin, Fe_3O_4@SiO_2, nanoparticle, doxorubicin, targeted tumor

Introduction

Doxorubicin (DOX), one of the most commonly used antitumor drugs, is a broad spectrum anticancer agent, used in therapy against solid tumors and hematopoietic malignancies.[1–2] However, serious side effects, including cardiomyopathy and congestive heart failure, have limited its clinical applications.[3–4] To decrease potential toxicities and improve its properties, the development of effective treatment methods for targeted drug delivery is of vital importance. In recent years, different superparamagnetic nanoparticles, modified with various surface coatings, have been widely applied in biomedical fields, including targeted drug delivery[5] and magnetic resonance imaging.[6] Delivering DOX under external magnetic field induction, for targeted chemotherapy, will allow it to preferentially remain at the site, thereby raising drug levels at the site of tumor, which could potentially maximize therapeutic effect, with minimal toxicity to healthy tissues.[7–9] For these kinds of clinical applications, high drug loading ability, suitable size, good dispersion, and low toxicity of particles are quite important. Magnetic particles coated with various surface layers, such as lipid,[10] polymer,[11–12] and micelle layers,[13] have been developed for targeted drug delivery, and have attained great success in biomedical applications. Recently, silica has been widely used in biomedical applications, because of its merits of high stability with respect to pH and concentration, easy functionalization, and biocompatibility.[14] Through silica surface modifications, magnetic nanoparticles can avoid agglomeration, improve stability, and facilitate connection with other functional groups; they show great potential for targeted drug delivery. However, because the content of functional groups in the

Correspondence: Lin Guo
Key Laboratory of Mesoscopic Chemistry of Ministry of Education, School of Chemistry and Chemical Engineering, Nanjing University, Nanjing 210093, People's Republic of China
Tel +86 25 8359 3262
Fax +86 25 8331 7761
Email linguo@nju.edu.cn

surface of nanoparticles is limited, drug loading efficiency is generally low (the drug loading percentage is less than 20%, in most cases). The low efficiency of drug loading requires use of a large amount of nanoparticle carrier. This may lead to several problems, such as toxicity, biodegradation, and metabolization of the nanoparticle carrier.[15]

Coupling particular ligands of therapeutic agents with nanoparticle carriers can enhance their antitumor activity, due to the strong bond between receptor-expressing tumor cells and the ligands, as well as the intracellular delivery potential of cell-mediated endocytosis.[16–17] Various ligands have been linked to nanoparticles for enhancing drug delivery efficiency.[18–20] Human serum transferrin is a single-chain glycoprotein, present in plasma, that can transport iron in the human body.[21] The transferrin receptor (TfR), also known as CD71, is usually overexpressed on the surfaces of proliferating cancer cells, due to their increased iron requirements.[22–24] Through receptor-mediated endocytosis, Tf easily enters the TfR-overexpressing cells. Consequently, it is widely used in targeting drug delivery, for improving cellular and nuclear uptake.

In the present study, we set out to develop a multifunctional Fe_3O_4@SiO_2-based drug delivery system that combines three properties: magnetic targeting, TfR targeting, and high DOX loading. A dual functional group, modified Fe_3O_4@SiO_2 nanoparticle (DMP) was synthesized as a carrier. Using a multifunctional coupling reagent, poly-L-glutamic acid (PLGA), DOX can be efficiently coupled to the DMP, through the PLGA single- to multi-amino groups method. Transferrin is used as a targeting ligand, and can also chemically conjugate to the carrier. Using this method, we have developed an efficient approach for generating transferrin-conjugated Fe_3O_4@SiO_2 nanoparticles, with high DOX loading, for dual-targeted anticancer drug delivery; we studied their structure and biomedical properties.

Materials and methods

Materials

Doxorubicin hydrochloride was obtained from Tongchuang Medicine Technology (Beijing, People's Republic of China). Transferrin, PLGA (molecular weight: 3,000–15,000 g/mol), N-hydroxysuccinimide (NHS), and N-(3-Dimethylaminopropyl)-N′-ethylcarbodiimide hydrochloride (EDC) were obtained from Sigma-Aldrich Company (St Louis, MO, USA). The Henrietta Lacks strain of cancer cells (HeLa) and human leukemia cell line K562 carcinoma cells were provided by the cell repository of the Chinese Academy of Sciences (Shanghai, People's Republic of China).

Synthesis of N-phthaloyl-L-glutamic acid anhydride (GA)

Equimolar quantities of phthalic anhydride and L-glutamic acid were mixed in a tube and reacted for 15 minutes. The product was recrystallized using ethanol–aqueous solution (9:1 v/v), and dried at 40°C for 24 hours, under vacuum. Then, 2.13 mL of acetic anhydride was added to the product obtained above, and refluxed for 15 minutes. The product, GA, was obtained after further recrystallization and drying at 40°C for 24 hours, under vacuum.

Generation of DMP

Superparamagnetic nanoparticles (Fe_3O_4) were obtained using the method reported by Stroeve et al.[25] The particle surface was then transformed into SiO_2 shell by a sol-gel process,[26] using tetraethyl orthosilicate. The product obtained was suspended in absolute ethanol containing ammonia solution. Then, 200 mg GA and 200 mg 3-aminopropyltrimethoxysilane were added. After the magnetite suspension had been sonicated for 5 minutes, the mixture was stirred at 40°C for 12 hours. The product was then washed three times with ethanol, and dried at 40°C, under vacuum.

Preparation of TfDMP

DMP was suspended in 10 mL phosphate-buffered saline (PBS) solution, and incubated with 5 mg EDC and 5 mg NHS for 30 minutes at room temperature. Then, the products were separated using magnetic separation and centrifugation. After washing once in PBS, the residual solution was mixed with 5 mg PLGA, then intermittently sonicated for 30 minutes at room temperature. The products were then magnetically separated, and washed three times. The residual solution was mixed with 5 mg EDC, 5 mg NHS, and 500 µL DOX (2 mg/mL). After intermittent sonication for 3 hours, the products were washed several times, until the supernatant solution became colorless. Then, 20 µL of hydrazine hydrate solution was added, and the mixture was incubated under impulse sonication for 10 minutes at room temperature. After being washed with PBS, 200 µL of transferrin solution (4 mg/mL), containing 5 mg EDC and 5 mg NHS, was added, and reacted under impulse sonication for 2 hours. The products were magnetically collected, then washed several times. TfDMP products were finally obtained by freeze-drying. Evaluation of DOX content proceeded by measuring the visual ultraviolet light absorbance of TfDMP at 479 nm, in a 1:2 mixture of hydrochloric acid and ethanol solution, as has been described in the literature previously.[27] The drug loading percentage (R) was calculated as: $R = D/(D + 1{,}000) \times 100\%$, where D is the amount of DOX coupled to DMP.

Transmission electron microscopy

Transmission electron microscopy (TEM) samples were prepared by deposition of a drop of nanoparticle precipitate solution onto a copper mesh grid, covered with a carbon film. TEM was recorded using a JEM-200CX microscope (JEOL, Tokyo, Japan).

Cellular uptake of TfDMP

A suspension of HeLa and K562 cells (1×10^4 cells) was seeded in a bottom-hole culture dish (0.13 mm glass) for 12 hours. For flow cytometry measurement, TfDMP, with a total DOX concentration of 2 μg/mL, was added to the cell culture dish and incubated for 1 hour at 37°C. After washing three times with PBS solution, the cancer cells were observed using an FACSCanto flow cytometer (BD Biosciences, San Jose, CA, USA). For confocal laser scanning microscopy measurement, TfDMP, with a total DOX concentration of 4 μg/mL, was added to the cell culture dish, then incubated for 2 hours at 37°C. After washing three times with PBS, the cancer cells were observed using an LSM 710 fluorescence microscope (Carl Zeiss Microscopy, Jena, Germany).

In vitro DOX release and MTT cytotoxicity studies

In vitro DOX release studies of TfDMP were carried out in test tubes at 37°C, under stirring conditions of 60 rpm. After incubation for a given time, TfDMP was magnetically separated. The supernates were diluted with 1:2 hydrochloric acid, and measured using a UV-7150 spectrophotometer (Shimadzu Corp, Kyoto, Japan). Then, the DOX content was obtained by using a standard curve: $c = 44.96\times A$, where c is the DOX concentration (μg/mL) and A is absorbance of supernates at 479 nm.

MTT cytotoxicity studies

MTT assays followed the procedure described by Bliss,[28] using both HeLa and K562 cells. All assays were carried out three times, with each sample in quintuplicate. TfDMP and DOX-coupled DMP (DDMP) were controlled to the same DOX concentration, using ultraviolet (UV) spectra, before being added to the cell solution. Then, certain volumes of TfDMP, DDMP, DMP, and Tf were added to the cell solution, which was incubated for a further 72 hours. The cell inhibition percentage was then calculated as follows:

$$\text{Cytotoxicity} = (1-[\text{absorbance of experimental wells}]/[\text{absorbance of control wells}])\times100$$

Results and discussion

The procedures for generation and drug loading of TfDMP are shown in Figure 1. By coupling GA with amino-immobilized Fe_3O_4@SiO_2, the surface of the magnetic nanoparticle can be modified with both carboxyl and protected amino groups. The dual function magnetic nanoparticles produced were used as carriers. As a multi-armed crosslinker, PLGA has large numbers of carboxyl functional groups, as well as an amino end-group. Thus, PLGA can couple with the carboxyl of DMP, in the presence of NHS and EDC, through an amide bond. Thereby, large numbers of carboxyl functional groups can be introduced onto the surface of DMP. It is known that DOX has an amino group, which is not the active site for DOX effectiveness. Thus, DOX can be immobilized (under vacuum) onto the PLGA-coated layer of the DMP, in the presence of NHS and EDC, through amide bonding. Finally, after deprotection of DMP's amino groups, Tf can be coupled, through amide bonding.

The structural properties of nanoparticle products at different steps of their synthesis are measured by attenuated total reflection infrared spectroscopy (Figure 2). As shown in Figure 2A, the peak around 580 cm^{-1} is assigned to the stretching vibration of the Fe–O band of Fe_3O_4. After coating DMP with a GA-modified SiO_2 layer, there appeared a new band at 1,108 cm^{-1}, assigned to the Si–O bond, proving the formation of the silica layer on the nanoparticles. Two peaks, at 1,775 cm^{-1} and 1,815 cm^{-1}, are owing to the carboxyl group of the acid anhydride (Figure 2B). Figure 2C shows that TfDMP has the Fe–O stretching vibration band at around 580 cm^{-1}, indicating that the product contains magnetite – Fe_3O_4. The band at 1,108 cm^{-1}, from the Si–O bond, verifies that the silica layer formed on nanoparticles. The presence of bands at 1,640 cm^{-1} and 1,577 cm^{-1} is due to the typical amide I and amide II bands of the transferrin protein (Figure 2E), which provides evidence of the transferrin modification.[29] The strong band observed at 1,730 cm^{-1} results from the stretching vibration of DOX's 13-carbonyl group (Figure 2D). The bond that appears at 1,284 cm^{-1} is due to framework vibration of the carbonyl group of DOX's anthracene cycle (Figure 2D). These bands confirmed that TfDMP contained DOX. Two peaks of DOX at 1,750–1,880 cm^{-1} (Figure 2B), assigned to the carboxyl group of acid anhydride, disappear after reaction (Figure 2C), indicating that Tf and DOX are mainly covalently bonded onto DMP.

TfDMP shows high DOX loading efficiency; the highest drug loading percentage is about 85%. This is about seven times the efficiency of lipid, micelle, or polymer carriers (approximately 12%),[30–32] and about two times that of bacteria

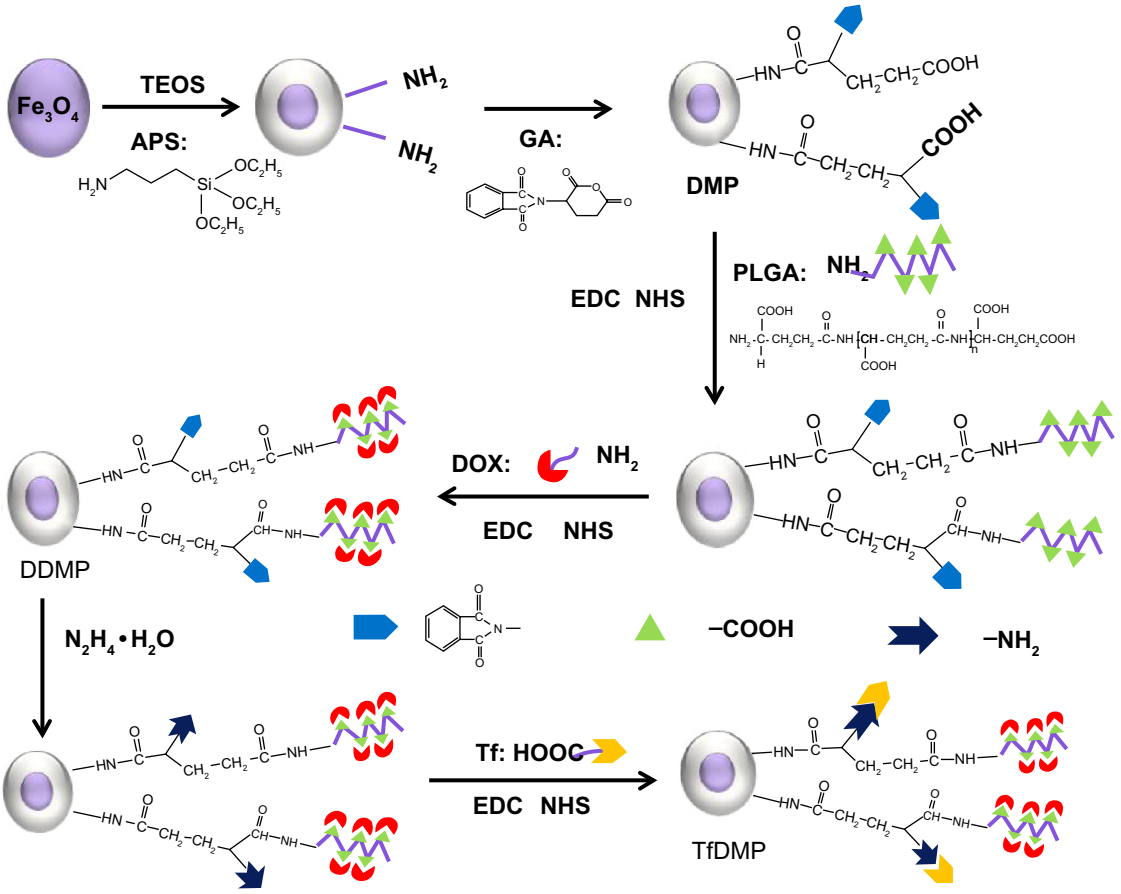

Figure 1 Route for generation of transferrin immobilized Fe_3O_4 magnetic nanoparticles with high doxorubicin load.
Abbreviations: TEOS, tetraethyl orthosilicate; APS, 3-aminopropyltrimethoxysilane; GA, N-phthaloyl-L-glutamic acid anhydride; PLGA, poly-L-glutamic acid; EDC, 1-ethyl-3-[3-dimethylaminopropyl]carbodiimide hydrochloride; NHS, N-hydroxysuccinimide; Tf, transferrin; DOX, doxorubicin; DMP, dual-function magnetic nanoparticle; DDMP, DOX-coupled DMP; TfDMP, DDMP with immobilized Tf.

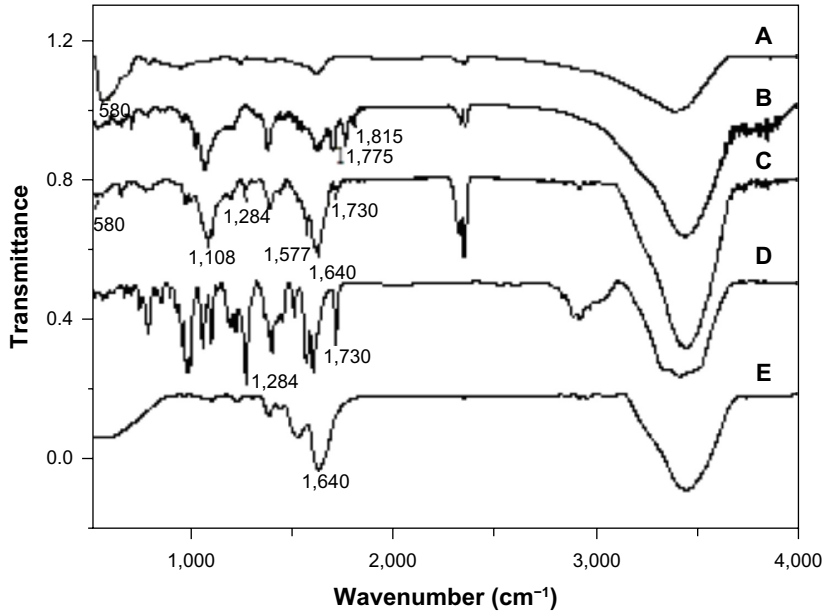

Figure 2 ATR-IR spectra.
Notes: (**A**) Fe_3O_4; (**B**) DMP; (**C**) TfDMP; (**D**) DOX; (**E**) Tf.
Abbreviations: ATR-IR, attenuated total reflection infrared; DMP, dual-function magnetic nanoparticle; DOX, doxorubicin; Tf, transferrin; TfDMP, DOX-coupled DMP with immobilized Tf.

magnetic particles formed using the dual-coupling reagent glutaraldehyde.[27] This efficiency is due to the much more functional positions provided by PLGA for loading DOX onto DMP. Enhanced drug loading is due to the increased number of functional "arms" on the DMP surface. More functional arms could provide more functional positions for DOX to load onto DMP. The DOX-to-DMP ratio (DOX/DMP) greatly influences DOX loading percentage (Figure 3). The drug loading percentage rises accordingly with increase of DOX/DMP. Coupling efficiency reaches its maximum when the DOX/DMP ratio equals 8. These results can be explained by the large number of carboxyl functional groups in the PLGA layer coating; more DOX can react with more carboxyl functional groups, leading to high loading efficiency. When available functional groups have been used up, maximum coupling efficiency is obtained, and coupling efficiency does not further increase. It is known that toxicity of conjugates would arise, due to excess nanoparticle dosage, if drug loading efficiency were low. Hence, a carrier with high drug loading ability can reduce toxic effects.[14] Consequently, TfDMP with low carrier toxicity can be generated, by adjusting the DOX/DMP ratio.

Magnetism and size

Figure 4A shows that TfDMP can be concentrated around a magnet when it is placed next to a cuvette; the bulk solution finally becomes colorless and transparent, confirming that TfDMP has a high magnetic response. The curve of magnetization versus field (Figure 4B) shows that TfDMP is superparamagnetic at room temperature, which is a significant property for a magnetic carrier.[7,33] There are no magnetic interactions between superparamagnetic

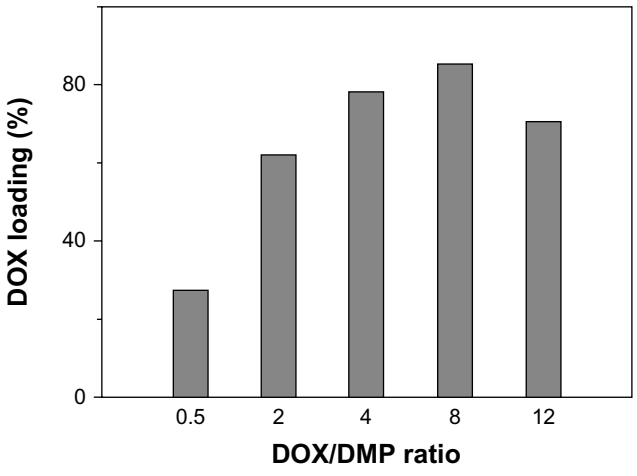

Figure 3 DOX loading percentage at different DOX/DMP ratios.
Abbreviations: DOX, doxorubicin; DMP, dual-function magnetic nanoparticle.

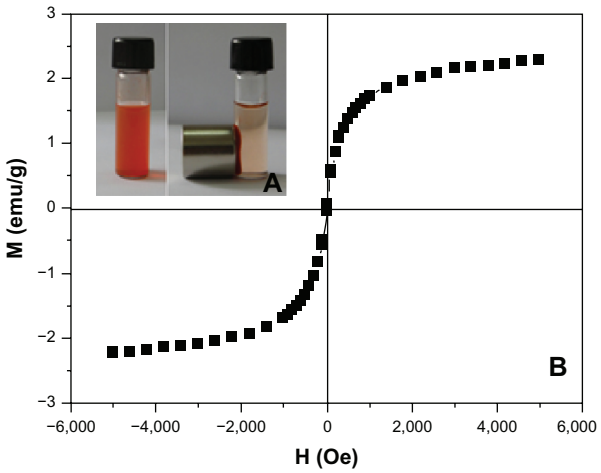

Figure 4 Magnetic properties of TfDMP.
Notes: (**A**) TfDMP suspended in aqueous solution before and 1 hour after a magnet is placed outside the test tube. (**B**) Magnetization versus field curve for TfDMP at 27°C.
Abbreviations: TfDMP, doxorubicin-coupled dual-function magnetic nanoparticle with immobilized transferrin; M, magnetization; emu, magnetic moment; H, field; Oe, oersted.

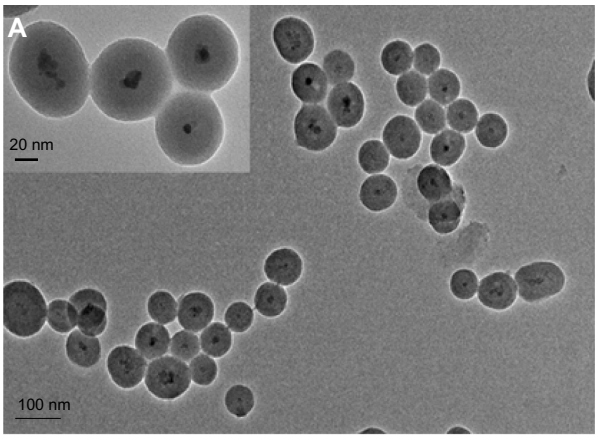

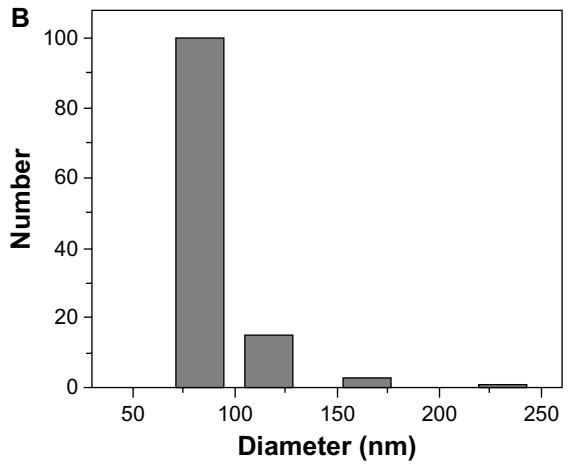

Figure 5 TfDMP characteristics.
Notes: (**A**) Transmission electron micrograph of TfDMP. (**B**) Size distribution plot of TfDMP, obtained by dynamic light scattering.
Abbreviation: TfDMP, doxorubicin-coupled dual-function magnetic nanoparticle with immobilized transferrin.

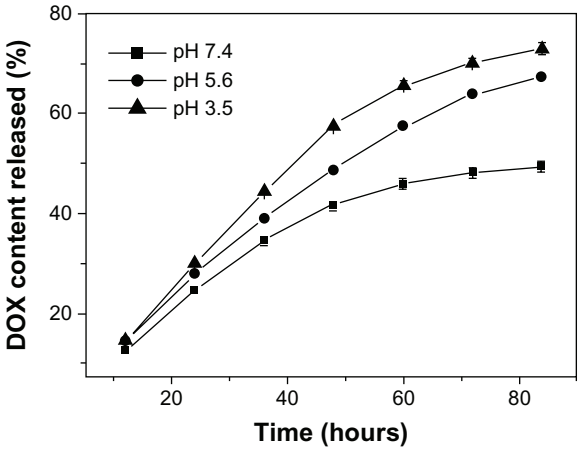

Figure 6 DOX release from TfDMP at different pH levels.
Note: TfDMP in phosphate-buffered saline solution at 37°C.
Abbreviations: DOX, doxorubicin; TfDMP, doxorubicin-coupled dual-function magnetic nanoparticle with immobilized transferrin; h, hours.

nanoparticles; therefore, minimal potential agglomeration, which reduces the danger of thrombosis in blood vessels. Its magnetic properties indicate that TfDMP can respond to an outer magnetic field; it has high trapping efficiency for magnetic targeting.

TEM (Figure 5A) reveals that TfDMP exhibits a core–shell structure. The core is composed of several magnetic nanoparticles <10 nm in diameter. This is the reason for the superparamagnetic property of TfDMP. We obtained the size distribution of TfDMP products by using dynamic light scattering. TfDMP exhibits a narrow particle size distribution (Figure 5B). The mean diameter of TfDMPs was determined to be approximately 90.8 nm. This value is similar to that obtained for TfDMP by TEM (Figure 5A), indicating that TfDMP disperses well and shows little agglomeration. The zeta potential of TfDMP at 25°C is about −44.1 mV. That TfDMP disperses well in aqueous solutions may be attributed to electrostatic repulsion of nanoparticles, and the screening effect of the covering of PLGA and silica.[34]

Drug release

TfDMP's drug release was measured under different pH conditions. Figure 6 shows that DOX release in weak acidic condition is quicker than that in neutral conditions. At pH 7.2 (which is similar to a normal physiological environment), TfDMP releases about 48% of its original DOX loading during incubation for 72 hours. The amount released increases to

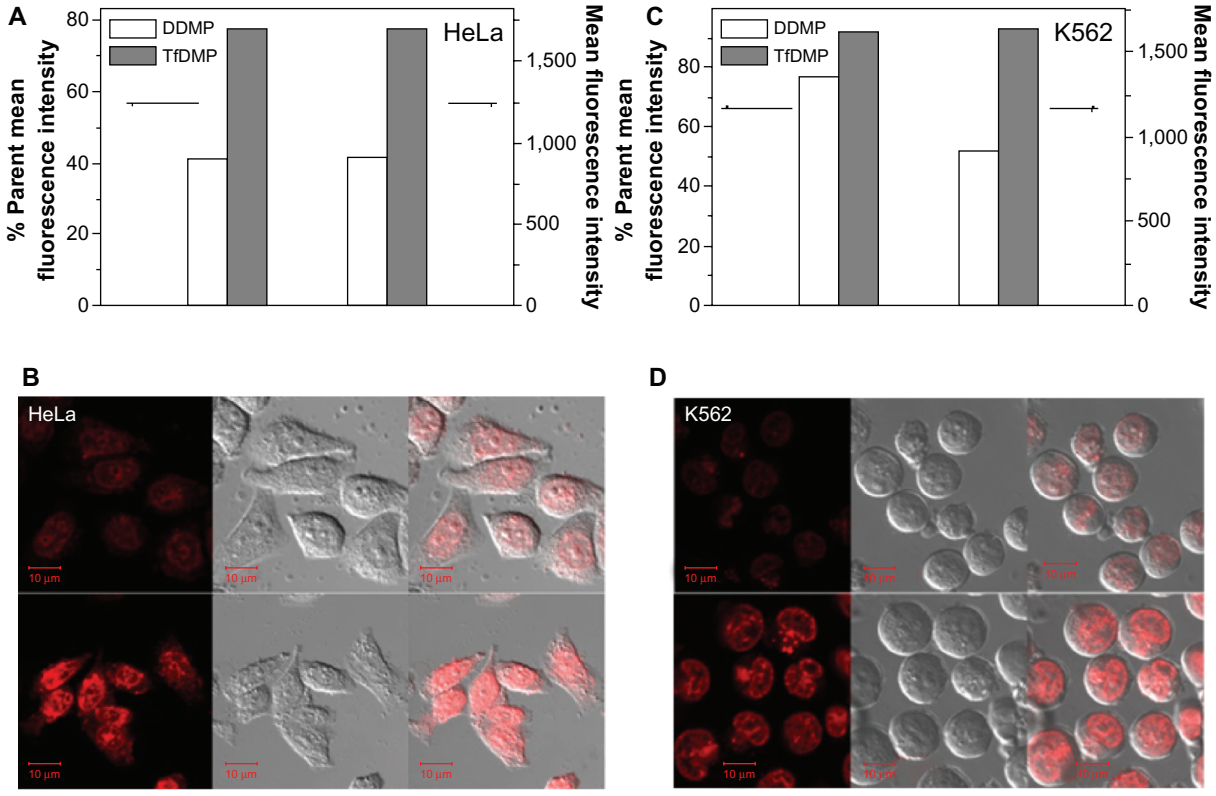

Figure 7 Comparison DDMP and TfDMP, with both cell lines.
Notes: Mean fluorescence intensity and parent percentage of (**A**) HeLa and (**C**) K562 cells after being incubated with DDMP and TfDMP for 1 hour, with a DOX concentration of 2 μg (by flow cytometry). Confocal laser scanning microscopy of (**B**) HeLa and (**D**) K562 cells treated with DDMP (upper) and TfDMP (lower), in the presence of a total DOX concentration of 4 μg/mL (after incubation for 2 hours at 37°C). Bars: 10 μm.
Abbreviations: DMP, dual-function magnetic nanoparticle; DOX, doxorubicin; DDMP, DOX-coupled DMP; TfDMP, DOX-coupled DMP with immobilized transferrin; HeLa, Henrietta Lacks strain of cancer cells; K562, human leukemia cell line.

63.7% at pH 5.6. The rate of DOX release increases accordingly with decreasing pH. These results may be explained by the following two reasons. First, the amide bonds between carboxylic groups of PLGA and DOX, as well as the amide bonds between carboxylic groups of nanoparticles and PLGA, become more unstable in acid solution. Second, protonation of amino groups in DOX, under acid conditions, speeds its release.[35] Due to these release properties, TfDMP releases more DOX in the mildly-acidic physiological environment of tumor than in the relatively neutral physiological environment of normal tissue. Taking advantage of its pH-sensitivity and release properties, TfDMP can be delivered systemically, for targeted delivery and release of drug to tumor.

Targeted uptake

The targeted uptake effect of TfDMP was evaluated both by confocal laser scanning microscopy (CLSM) and flow cytometry. Two lines of TfR-expressing cancer cells (HeLa and K562), were incubated with nanoparticles. Figure 7A and C show the mean fluorescence intensity and the parent ratio of cancer cells, after incubation with TfDMP, and DOX-coupled DMP (without Tf modification) (DDMP), respectively. It is observed that TfDMP shows a higher mean fluorescence intensity than DDMP. An increased uptake was observed with TfDMP, compared with DDMP – approximately 1.9 times greater in HeLa cells, and 1.2 times greater in K562 cells. The intracellular distribution and uptake of TfDMP and DDMP were also measured by CLSM. It can be seen from Figure 7B and D that the majority of nanoparticles were localized in cytoplasmic compartments (eg, endosomes), once taken into cancer cells. The intracellular DOX fluorescence intensity of TfDMP is higher than that of DDMP, indicating a greater uptake of TfDMP by cancer cells. Flow cytometry results were in agreement, indicating enhanced cellular uptake of TfDMP, compared with DDMP. This may be because rapid TfR-mediated endocytosis facilitates internalization of TfDMP by cancer cells.

Antitumor effects

The antitumor effects of TfDMP were tested using TfR-expressing K562 and HeLa cells. Samples of TfDMP and DDMP were controlled to the same DOX concentration (using UV spectra) before being added to the cell solution, which was then incubated for 72 hours. The cell inhibition ratio was computed by calculating the ratio of cell numbers between the treated group and the untreated controls. Figure 8 displays that free DMP, or pure Tf, produces little inhibition of cell growth, indicating low

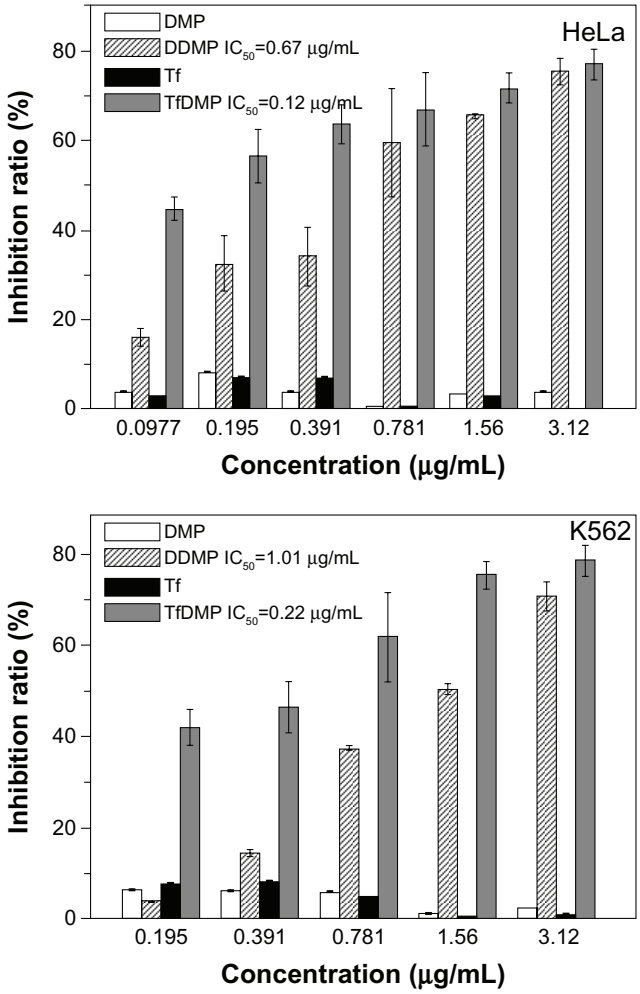

Figure 8 Cytotoxic effects of DMP, DDMP, Tf, and TfDMP, in HeLa and K562 cells.
Abbreviations: DMP, dual-function magnetic nanoparticle; DDMP, doxorubicin-coupled DMP; TfDMP, doxorubicin-coupled DMP with immobilized transferrin, Tf, transferrin; IC_{50}, half maximal inhibitory concentration; HeLa, Henrietta Lacks strain of cancer cells; K562, human leukemia cell line.

cytotoxicity for both Tf and the DMP carrier. The TfDMP we prepared shows high cytotoxicity to tumor cells; it inhibited the proliferation of tumor cells efficiently. These results indicate that our DOX-coupling method is effective. In comparison to DDMP without Tf modification, TfDMP exhibited higher cytotoxicity to tumor cells, at the same DOX concentration. A lower half maximal inhibitory concentration (IC_{50}) value is found for TfDMP than for DDMP. These results demonstrate an increased drug delivery effect in receptor-targeted uptake of TfDMP by TfR-expressing cancer cells.

Conclusion

Transferrin-conjugated Fe_3O_4@SiO_2 nanoparticles, with high DOX loading (TfDMP) were produced, for the dual-targeting of cancer. TfDMP exhibit three merits: 1) high trapping efficiency for magnetic targeting, which can be attributed

to its superparamagnetic core; 2) Tf-receptor-targeting, by the Tf ligand on the outer layer; and 3) high drug loading efficiency (achieved using a modified multi-armed coupling reagent, PLGA), controllable by altering reactant proportions. Moreover, TfDMP exhibited a narrow particle size distribution and showed pH-dependent release characteristics. Compared with DOX-coupled nanoparticles without a Tf modification, there was enhanced uptake of TfDMP by TfR-expressing tumor cells, and a stronger cytotoxicity was observed. This investigation reveals an effective method for dual-targeted delivery of chemotherapeutic agents to tumors, with greater control, low carrier toxicity, and high efficiency.

Acknowledgment

We thank the Natural Science Foundation of China (Project No NSFC21073091).

Disclosure

The authors report no conflicts of interest in this work.

References

1. Minotti G, Menna P, Salvatorelli E, Cairo G, Gianni L. Anthracyclines: molecular advances and pharmacologic developments in antitumor activity and cardiotoxicity. *Pharmacol Rev*. 2004;56(2):185–229.
2. Pollakis G, Goormaghtigh E, Ruysschaert JM. Role of the quinine structure in the mitochondrial damage induced by antitumor anthracyclines. Comparison of adriamycin and 5-iminodaunorubicin. *FEBS Lett*. 1983;155(2):267–272.
3. Singal PK, Iliskovic N. Doxorubicin-induced cardiomyopathy. *N Engl J Med*. 1998;339(13):900–905.
4. Singal PK, Iliskovic N, Li T, Kumar D. Adriamycin cardiomyopathy: pathophysiology and prevention. *FASEB J*. 1997;11(12):931–936.
5. Kong SD, Zhang WZ, Lee JH, et al. Magnetically vectored nanocapsules for tumor penetration and remotely switchable on-demand drug release. *Nano Lett*. 2010;10:5088–5092.
6. Olariu CI, Yiu HHP, Bouffier L, et al. Multifunctional Fe3O4 nanoparticles for targeted bi-modal imaging of pancreatic cancer. *J Mater Chem*. 2011;21:12650–12659.
7. Arruebo M, Fernández-Pacheco R, Ibarra MR, Santamaría J. Magnetic nanoparticles for drug delivery. *Nano today*. 2007;2(3):22–32.
8. Alexiou C, Arnold W, Klein RJ, et al. Locoregional cancer treatment with magnetic drug targeting. *Cancer Res*. 2000;60(23):6641–6648.
9. Babincova M, Altanerova V, Altaner C, Cicmanec P, Babinec P. In vivo heating of magnetic nanoparticles in alternating magnetic field. *Med Phys*. 2004;31(8):2219–2221.
10. Brulé S, Levy M, Wilhelm C, et al. Doxorubicin release triggered by alginate embedded magnetic nanoheaters: a combined therapy. *Adv Mater*. 2011;23(6):787–790.
11. Mikhaylov G, Mikac U, Magaeva AA, et al. Ferri-liposomes as an MRI-visible drug-delivery system for targeting tumours and their microenvironment. *Nat Nanotechnol*. 2011;6(9):594–602.
12. Gaihre B, Khilb MS, Lee DR, Kim HY. Gelatin-coated magnetic iron oxide nanoparticles as carrier system: drug loading and in vitro drug release study. *Int J Pharm*. 2009;365(1–2):180–189.
13. Yu JM, Xie X, Zheng M, et al. Fabrication and characterization of nuclear localization signal-conjugated glycol chitosan micelles for improving the nuclear delivery of doxorubicin. *Int J Nanomedicine*. 2012;7:5079–5090.
14. El-Gamel NE, Wortmann L, Arroub K, Mathur S. SiO_2@Fe_2O_3 core-shell nanoparticles for covalent immobilization and release of sparfloxacin drug. *Chem Commun (Camb)*. 2011;47(6):10076–10078.
15. Allen TM, Cullis PR. Drug delivery systems: entering the nainstream. *Science*. 2004;303(5665):1818–1822.
16. Peer D, Karp JM, Hong S, Farokhzad OC, Margalit R, Langer R. Nanocarriers as an emerging platform for cancer therapy. *Nat Nanotechnol*. 2007;2(12):751–760.
17. Pearce TR, Shroff K, Kokkoli E. Peptide targeted lipid nanoparticles for anticancer drug delivery. *Adv Mater*. 2012;24(28):3803–3822, 3710.
18. Park JW, Hong K, Kirpotin DB, et al. Anti-HER2 immunoliposomes: enhanced efficacy attributable to targeted delivery. *Clin Cancer Res*. 2002;8(4):1172–1181.
19. Yu MK, Park J, Jeong YY, Moon WK, Jon S. Integrin-targeting thermally cross-linked superparamagnetic iron oxide nanoparticles for combined cancer imaging and drug delivery. *Nanotechnology*. 2010;21(41):415102.
20. Toublan FJJ, Boppart S, Suslick KS. Tumor targeting by surface-modified protein microspheres. *J Am Chem Soc*. 2006;128(11):3472–3473.
21. Indira Chandran V, Matesic L, Locke JM, Skropeta D, Ranson M, Vine KL. Anti-cancer activity of an acid-labile N-alkylisatin conjugate targeting the transferrin receptor. *Cancer Lett*. 2012;316(2):151–156.
22. Daniels TR, Delgado T, Rodriguez JA, Helguera G, Penichet ML. The transferrin receptor part I: biology and targeting with cytotoxic antibodies for the treatment of cancer. *Clin Immunol*. 2006;121(2):144–158.
23. Daniels TR, Delgado T, Helguera G, Penichet ML. The transferrin receptor part II: targeted delivery of therapeutic agents into cancer cells. *Clin Immunol*. 2006;121(2);159–176.
24. Peng JL, Wu S, Zhao XP, et al. Downregulation of transferrin receptor surface expression by intracellular antibody. *Biochem Biophys Res Commun*. 2007;354(4):864–871.
25. Kang YS, Risbud S, Rabolt JF, Stroeve P. Synthesis and characterization of nanometer-size Fe_3O_4 and γ-Fe_2O_3 particles. *Chem Mater*. 1996;8(9):2209–2211.
26. Liu X, Ma Z, Xing J, Liu H. Preparation and characterization of amino-silane modified superparamagnetic silica nanospheres. *J Magn Magn Mater*. 2004;270(1–2):1–6.
27. Guo L, Huang J, Zhang X, Li Y, Zheng L. Bacterial magnetic nanoparticle as a drug carrier. *J Mater Chem*. 2008;18:5993–5997.
28. Bliss C. The calculation of the dose-mortality curve. *Ann Appl Biol*. 1935;22:134–167.
29. Ciofani G, Del Turco S, Genchi GG, D'Alessandro D, Basta G, Mattoli V. Transferrin-conjugated boron nitride nanotubes: protein grafting, characterization, and interaction with human endothelial cells. *Int J Pharm*. 2012;436(1–2):444–453.
30. Du W, Xu Z, Nystrom AM, Zhang K, Leonard JR, Wooley KL. 19F- and fluorescently labeled micelles as nanoscopic assemblies for chemotherapeutic delivery. *Bioconjug Chem*. 2008;19(12):2492–2498.
31. Guo S, Li D, Zhang L, Li J, Wang E. Monodisperse mesoporous superparamagnetic single-crystal magnetite nanoparticles for drug delivery. *Biomaterials*. 2009;30(1):1881–1889.
32. Hu Y, Xie J, Tong YW, Wang CH. Effect of PEG conformation and particle size on the cellular uptake efficiency of nanoparticles with the HepG2 cells. *J Control Release*. 2007;118(1):7–17.
33. Meza Mary. Chapter 22: Application of magnetic particles in immunoassays. In: Hafeli U, Schutt W, Zborowski M, editors. *Scientific and Clinical Applications of Magnetic Carriers*. New York: Plenum; 1997:303–310.
34. Xu X, Deng C, Gao M, Yu W, Yang P, Zhang X. Synthesis of magnetic microspheres with immobilized metal ions for enrichment and direct determination of phosphopeptides by matrix-assisted laser desorption ionization mass spectrometry. *Adv Mater*. 2006;18(24):3289–3293.
35. Sahu SK, Maiti S, Pramanik A, Ghosh SK, Pramanik P. Controlling the thickness of polymeric shell on magnetic nanoparticles loaded with doxorubicin for targeted delivery and MRI contrast agent. *Carbohydr Polym*. 2012;87(4):2593–2604.